Check for updates

Potentially toxigenic phytoplankton patterns in the northwestern Iberian Peninsula

Amália Maria Sacilotto Detoni[1]*, Gabriel Navarro[1],
Xosé Antonio Padín[2], Eduardo Ramirez-Romero[1],
Maria Laura Zoffoli[3], Yolanda Pazos[4] and Isabel Caballero[1]

[1]Instituto de Ciencias Marinas de Andalucía (ICMAN), Consejo Superior de Investigaciones Científicas (CSIC), Puerto Real, Spain, [2]Instituto de Investigaciones Marinas, Consejo Superior de Investigaciones Científicas (IIM, CSIC), Vigo, Spain, [3]Consiglio Nazionale delle Ricerche, Istituto di Scienze Marine (CNR-ISMAR), Rome, Italy, [4]Instituto Tecolóxico para o Control do Medio Mariño de Galicia (INTECMAR), Peirao de Vilaxoán, Villagarcía de Arosa, Spain

The Galician estuaries are Europe's foremost supplier of mussels, generating millions of euros annually and offering substantial employment opportunities for its population. One of the most critical threats to shellfish production is the occurrence of harmful algal blooms (HABs), contaminating bivalves with phytotoxins. To successfully tackle this problem, there needs to be a collaborative effort between the scientific community and decision-makers to establish a dynamic and effective monitoring system. This could enable early warnings and preventive actions to avert the loss of millions of tons of shellfish. Remote sensing, despite its limitations, requires commitment and effort by experts to devise effective methods for detecting target optical constituents mixed with other undesired target but that exhibit strong signals. Therefore, the essential necessity arises to identify approaches for mitigating the shortcomings of the undertaken efforts. The objective of this study is to assess the main environmental drivers of potential harmful genera (*Pseudo-nitzschia*, *Dinophysis*, *Alexandrium*, and *Gymnodinium*) in the Rías Baixas from 2015 to 2022, developing regression-based models and customizing Generalized Additive Models (GAMs) to investigate their spatial-temporal dynamics. Risk-susceptible bloom zones were identified in the river mouth of the Ría Pontevedra and from the center to offshore of the Ría Vigo. Early upwelling events triggered peaks in chlorophyll-a (Chl-a), driving *Dinophysis* grazing on phytoplankton communities mainly dominated by diatoms, flagellates, and ciliates. Subsequently, the upwelling intensity favoring *Pseudo-nitzschia* or *Alexandrium minutum* growth as larger diatoms declined. *A. minutum* exhibited elevated incidence over the past five years. *Gymnodinium catenatum* presented a rare occurrence across the three studied estuaries, which limited the assessment of its spatial dynamics in the region. This study emphasizes the need to integrate remote sensing evaluation of high-risk bloom areas (July to September), *in-situ* cell count collection, and enhanced efforts for forecasting future critical occurrences of HABs.

Highlights

- Occurrences of *Pseudo-nitzschia* followed by the presence of *Dinophysis*.
- Susceptible areas and environmental conditions that favor HABs were identified.
- GAM analysis identified key environmental factors promoting HABs.
- *A. minutum* cell density linked to temperature, stratification, and river flow.

1 Introduction

The Galician region, in the northernmost limit of the Canary Current Upwelling System (NW of the Iberian Peninsula) is highly productive (Arístegui et al., 2009) in terms of extensive shellfish farming (mussels, oysters, and clams). This productivity is primarily attributed to important oceanographic processes, such as wind-driven upwelling events, river discharges, and mesoscale eddies. These processes promote seawater fertilization and abundant phytoplankton production, which in turn, provides crucial support for a substantial number of aquiculture facilities, making this region a world leader in mussel production (Álvarez-Salgado et al., 2000; Figueiras et al., 2002; Labarta and Fernández-Reiriz, 2019). Mussel farms along the Galician coast are predominantly concentrated in the large estuaries of the southern region known as the Rías Baixas, contributing to 93% of the entire mussel production in Galicia (https://www.pescadegalicia.gal/Publicaciones/AnuarioAcuicultura2022/Informes/5.1.6.html).

The phytoplankton community composition in the Galician estuaries is influenced by the hydrographic variability imposed by upwelling-downwelling dynamics (Figueiras et al., 2002). Upwelling events inject nutrients into the euphotic zone and are more frequent during spring and autumn on the coast of NW Spain, induced by northerly winds (Díaz et al., 2014; Díaz et al., 2016; Palenzuela et al., 2019). They start to become relatively weak in late summer (Figueiras et al., 2020). Other important oceanographic processes are the upwelling and downwelling relaxation events, which are driven by small fluctuations in the large-scale climatology of the North Atlantic and favored by the weakening of winds that induce upwelling and downwelling (Álvarez et al., 2012). During these events, reduced winds and increased solar radiation can lead to water column stratification, consequently impacting plankton composition and size structure, creating ideal conditions for the proliferation of certain toxic phytoplankton species, resulting in the formation of Harmful Algae Blooms (HABs) (Froján et al., 2014). Previous studies have demonstrated that in the southern Galician estuaries, the annual phytoplankton succession fellows a clear temperature-marine seasonal pattern superimposed by short-term (1-2 weeks) and annual variability of the upwelling regime (Nogueira et al., 1997). Overall, during the upwelling conditions, diatoms dominate the phytoplankton population in the interior of the Rías Baixas and dinoflagellates are located towards the shelf, associated with the upwelling fronts (Tilstone et al., 1994). When

the upwelling relaxes, the dinoflagellates located in the offshore waters are advected towards the estuaries and are accumulated under downwelling conditions (Escalera et al., 2010).

Recurrent HABs in the area lead to lengthy harvesting closures (Álvarez-Salgado et al., 2008), threaten food security, and have the potential to cause devastating economic losses in the shellfish aquaculture and fisheries industries (Zohdi and Abbaspour, 2019). The European losses have been quantified at up to 200 million euros per year (Scatasta et al., 2003). Although this analysis has not yet been conducted for Galicia in sufficient detail (Rodríguez et al., 2011), there is a consensus among producers, management, and researchers about the significant economic impact of mussel rafts closures due to HABs. This impact is notably evidenced through closures of shellfisheries and aquaculture activities, along with restrictions on the commercial sale of recreational fish (Hoagland and Scatasta, 2006).

Coastal and shallow areas are of major economic and social importance, besides their ecological and environmental value. There are several policies in Europe addressing the restoration and protection of waters in areas that are affected by anthropogenic pressures and intense production activities (Carvalho et al., 2019). Regulatory monitoring of harmful species in the water column and toxin concentrations within shellfish is currently the main means of warning of toxin levels in bivalves, with harvesting being suspended when toxicity is elevated above EU regulatory limits (Fernandes-Salvador et al., 2021). An increase of both frequency and intensity of phytoplankton blooms is expected in the coming decades across coastal and shallow areas due to global warming and increased coastal eutrophication (Anderson et al., 2019; Johansen et al., 2022). Monitoring and predicting HABs are crucial for early warnings and preventive measures, aimed at mitigating their environmental and economic impacts in coastal zones. Traditional monitoring networks have primarily relied on periodic *in-situ* sampling of the cell density of potentially toxic phytoplankton groups and toxins in the shellfish. This approach, however, has inherent spatial limitations and is confined to pre-scheduled sampling days (Anderson et al., 2019; Fernandes-Salvador, 2021). In this context, remote sensing could contribute to overcome these constraints. Nevertheless, it introduces its own set of challenges, such as cloud cover, uncertainties caused by the atmosphere, contamination of images due to sunglint, as well as frequent difficulties to identify many harmful phytoplankton (Martinez-Vicente et al., 2020; Johansen et al., 2022).

In order to highlight locations with elevated risk of HAB occurrences within the Rías Baixas, we assessed the coupling times series, spanning from 2015 to 2022, of environmental variables and *in-situ* phytoplankton cell count for a potential toxic diatom genera, *Pseudo-nitzschia* spp. (some species of which are potential producers of the neurotoxin domoic acid), a toxic dinoflagellate genera, *Dinophysis* spp. (producer of lipophilic shellfish toxins), and two toxic dinoflagellates species: *Alexandrium minutum* and *Gymnodinium catenatum* (producers of paralytic shellfish toxins). This approach aimed to enhance our understanding of the dynamics and succession of these key genera within the Galician marine ecosystem. In this context, our study can guide remote sensing experts in concentrating their efforts on zones and temporal intervals that manifest the most notable occurrences of blooms and favorable trends, which involve potential risks to society and mussel production.

2 Methods

2.1 Study area

The Rías Baixas are V-shaped coastal embayments along the Galician southern coast. This study focuses on three estuaries (Arousa, Pontevedra, and Vigo, Figure 1), which are connected to the North Atlantic Ocean and receive the contribution of freshwater input by rivers located in the innermost part of them. These estuaries are characterized by a mesotidal and a semidiurnal tide, which is the principal factor of their dynamics. Typical tidal amplitudes of 2 and 3 m were measured during neap and spring tides, respectively (DeCastro et al., 2000). Inside the Rías Baixas, the oceanographic dynamics are modulated mainly by a predominant positive residual circulation pattern driven by buoyancy currents (*i.e.*, estuarine-like) and the seasonal occurrence of upwelling events from April to September (Pardo et al., 2011). Notably, the oceanographic dynamics inside the Rías Baixas exhibit an opposing circulation pattern during downwelling events from October to March. Intermittently, concurrent with varying wind intensity and direction, cyclical episodes of upwelling relaxation occur (Cruz et al., 2021). Intense freshwater river discharges are commonly associated with heavy rains occurring in the Galician region typically from October to April (Otero et al., 2010).

2.2 *In-situ* sampling of potential harmful phytoplankton cell density and chlorophyll-a

Seawater samples were collected weekly from the surface to 15 m depth (integrated samples) with a flexible tube (integrated tube sampler) from January 2015 to December 2022, along the three estuaries at a total of 29 fixed stations (10 stations in Arousa, 11 in Pontevedra, and 8 in Vigo, Figure 1). Water samples were processed by the Technological Institute for the Control of the Marine Environment of Galicia, (Instituto Tecnolóxico para o Control do Medio Mariño de Galicia - INTECMAR) to quantify chlorophyll-a concentration (Chl-a) with the fluorometric method (Neveux and Panouse, 1987) (number of samples 8637), and cell counts of four phytoplankton genera that include potentially toxic species (number of samples 16529): one chain-forming diatom genus, *Pseudo-nitzschia* spp., and three dinoflagellates, the large cell *Dinophysis* spp., and two chain-forming *Alexandrium minutum*, and *Gymnodinium catenatum*. Cell counts were obtained using an inverted microscope at 100x magnification. The total biovolume per genus was calculated to evaluate the relative representativeness of cell biovolume concerning the diversity of cell size and shape for each evaluated taxon. Biovolume was computed by multiplying cell counts (cells·L^{-1}) by the average cellular volume per species. The average cellular volumes used were: *Pseudo-nitzschia* spp. - 997 μm^3, *Dinophysis* spp. - 31459 μm^3, *Alexandrium minutum* - 7200 μm^3, and *Gymnodinium catenatum* - 9333 μm^3 (Fariñas et al., 2017). Overall, the merging of phytoplankton cell counts, and Chl-a resulted in a total of 8278 matched samples.

2.3 Environmental datasets

Hydrological features came from CTD (conductivity, temperature, and pressure) cast from INTECMAR monitoring stations (http://www.intecmar.gal/Ctd/Default.aspx) (Figure 1). CTD raw casts were averaged firstly at 1 m intervals and then only using the 0 – 15 m layer. Riverine input data ($m^3 \cdot s^{-1}$) were
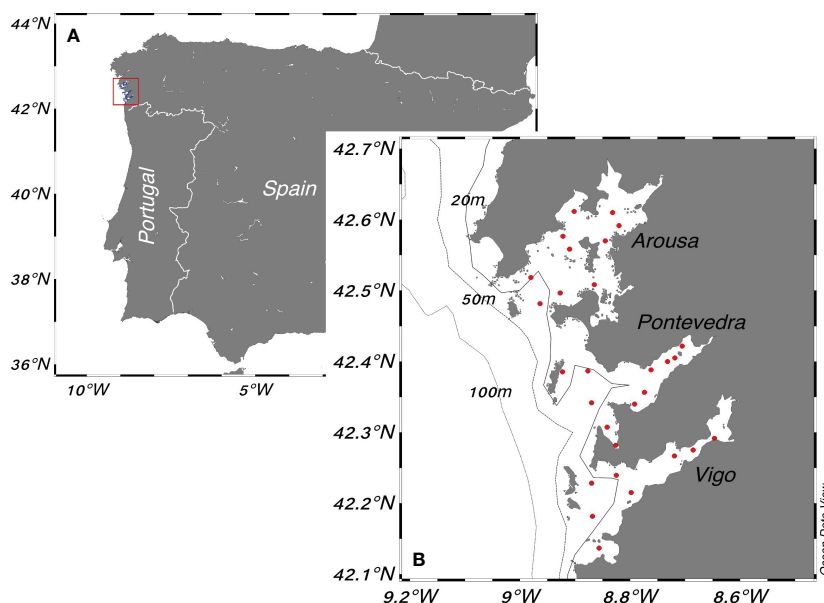

FIGURE 1
The Rías Baixas sampling area. **(A)** The Iberian Peninsula. The red rectangle represents the sampling area shown in panel **(B)**. **(B)** The sampling area. The red dots are the sampling stations of the Galician monitoring program (INTECMAR - http://www.intecmar.gal/Ctd/Default.aspx).

obtained from the MeteoGalicia website (http://www2.meteogalicia.gal/servizos/AugasdeGalicia/estacions.asp?request_locale=gl#) for the main rivers in Arousa (River Ulla), Pontevedra (River Lérez), and Vigo (River Verdugo). We constrained the biological *in-situ* dataset to the period when environmental variables were available (January/2015 – December/2022). The match (Chl-a, phytoplankton samples and environmental variables) was based on the sampling station and date. Only rows without gaps were used. As a result, we ended up with a total of 6358 samples.

The Brunt-Väisälä frequency (*N*) (Equation 1) was computed using CTD profile data, where ρ represents density at depth z and g denotes gravitational acceleration. A higher N value indicates a notable density gradient and substantial stratification. Consequently, the upper mixed layer depth (MLD) was determined at the depth of the first stratification maximum.

$$N = \sqrt{-\frac{g}{\rho}\frac{d\rho}{dz}} \qquad (1)$$

The daily upwelling index (UI) ($m^3 s^{-1} km^{-1}$) dataset off the Rías Baixas was downloaded from the Spanish Institute of Oceanography (http://www.indicedeafloramiento.ieo.es/index_UI_es.html, historical FNMOC reanalysis) (González-Nuevo et al., 2014). The UI represents the offshore Ekman flux in the surface layer, positive (negative) values indicate favorable conditions for upwelling (downwelling) process.

2.4 Statistical analyses

Besides an initial data exploration analysis of time series and spatial distribution, Canonical Correspondence Analysis (CCA) was applied to investigate the relationships between phytoplankton abundance and environmental variables in the dataset. This multivariate technique is commonly used to explore the influence of environmental factors on harmful phytoplankton distribution patterns, identifying the key environmental factors that drive this distribution. The method seeks linear combinations of the environmental variables that best explain the variation in genera densities (Legendre and Legendre, 1998). The resulting canonical axes (axes 1 and 2) provide a representation of each genus's responses to environmental gradients. The Monte Carlo permutation test was also applied to assess the statistical significance of the canonical axes. Water temperature, salinity, MLD, riverine inputs, UI, month (indicating the seasonal variability), latitude (as an indicator of spatial variability), and Chl-a were included in the CCA as explanatory variables. Chl-a is not an environmental variable *per se* but reflects the trophic conditions of the marine environment. Therefore, in this study, we use the Chl-a as an indicator of the phytoplankton community's total biomass in the explanatory/environmental variables.

A GAM analysis was conducted to explore the connections between phytoplankton genus cell density (response variables) and explanatory variables (environmental variables: salinity, temperature, UI, river flow, MLD, months, and latitude; and the

Chl-a as an indicator of the phytoplankton total biomass). This statistical approach is widely used for investigating non-linear relationships and potential interactions between response variables and predictors (Wood, 2000; Wood, 2006). Cell densities were normalized using a logarithmic transformation [Log10(x+1)]. The explanatory variables were examined for collinearity using Pearson's correlation coefficient ($r > 0.6 – 0.7$), and by calculating the concurvity (the GAM equivalent of collinearity) (Wood, 2017). For the estimate concurvity the reference value was taken to be< 0.6 to indicate that each explanatory variable is independent of the others. Then, GAMs were estimated for each phytoplankton group. Individual model selection was based on a both backward and forward step-wise approach removing covariates with a *p*-value > 0.05 (Table 1). The variable providing the best fit was chosen according to Akaike's information criterion (AIC) (Akaike, 1974), where the selected model has the lowest values of AIC. For validation purposes, the models were used to hindcast the observations. The analyses were performed using the statistical and programming software R 4.3.1 (R Core Team, 2012), package "mgcv" (Wood, 2006) available through the CRAN repository (www.r-project.org/).

3 Results

3.1 Relations between the studied phytoplankton genera and Chl-a patterns

Averaged Chl-a showed maxima (> 4 mg·m^{-3}) in the Ría Arousa (the northernmost) and in the innermost part of each estuary (Figure 2A). However, concerning the cellular biovolume product and cell concentrations for each genus, the lowest relative abundances ($< 3 \cdot 10^7$ µm^3·L^{-1}) were observed in the Ría Arousa for all four evaluated genera (Figures 2B–E). *Dinophysis* spp., one of the most toxic genera of phytoplankton, exhibited higher average relative abundance in the central part of the Ría Vigo ($\sim 1.7 \cdot 10^7$ µm^3·L^{-1} and cell density mean 220 ± 650 cells·L^{-1}) (Figure 2B). However, the diatom *Pseudo-nitzschia* spp. displayed the highest mean relative abundance ($> 4.2 \cdot 10^7$ µm^3·L^{-1} and cell density mean $4 \cdot 10^4$ ± $2 \cdot 10^5$ cells·L^{-1}) surpassing the other three examined genera. The elevated abundances were notably observed in the following estuary's locations: at the river mouth of the Ría Pontevedra and

TABLE 1 Summary of model statistics per phytoplankton genera *Pseudo-nitzschia* spp. (Pseu), *Dinophysis* spp., (Dino), *Alexandrium minutum* (Alex), and *Gymnodinium catenatum* (Gymn).

HABs	r^2	Dev. Expl.	N presence	N absent	AIC
Pseu	0.47	47%	3318	3040	24268
Dino	0.31	25%	3429	2929	16812
Alex	0.15	16%	298	6060	14660
Gymn	0.15	50.0%	277	6081	2729

The R-squared (r^2), deviance explained (Dev. Expl.), numbers of cell presence observations (N presence) and cell absence (N absent), and Akaike Information Criterion (AIC).
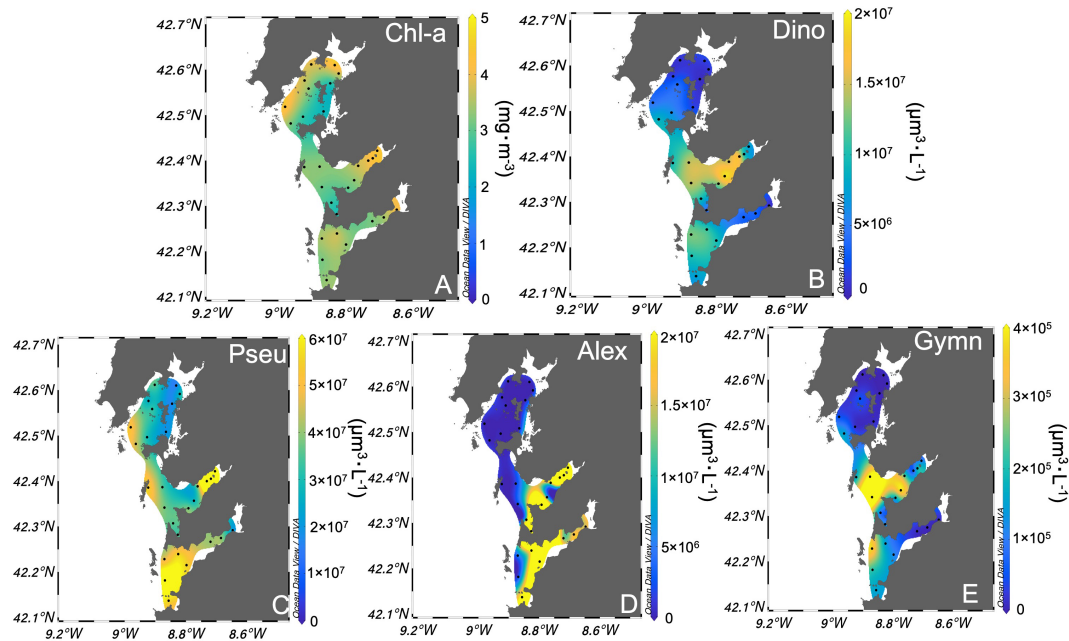
FIGURE 2
Surface distribution of the averages of weekly sampling from 2015 to 2022 of **(A)** chlorophyll-a concentration (Chl-a) (mg·m^{-3}), and cell biovolume (µm^3·L^{-1}) of **(B)** *Dinophysis* spp., **(C)** *Pseudo-nitzschia* spp., **(D)** *Alexandrium minutum* and **(E)** *Gymnodinium catenatum*. Be aware of the need to discern the color scale variations corresponding to each genus's cell biovolume magnitude.

across the majority of Ría Vigo's domain (Figure 2C). *A. minutum* ranked as the second most abundant group (> 2.2·10^7 µm^3·L^{-1} in the Rías Pontevedra and Vigo, and cell density mean 3·10^3 ± 4·10^4 cells·L^{-1}), with high densities also observed at river mouths in the Ría Pontevedra and the inner part of the Ría Vigo (Figure 2D). *G. catenatum* exhibited the lowest average relative abundance (< 10^7 µm^3·L^{-1} and cell density mean 16 ± 112 cells·L^{-1}) among the four evaluated genera across the three estuaries (Figure 2E).

Both the Chl-a and cellular density of the assessed genera displayed pronounced interannual variability (Figure 3). Throughout the entire *in-situ* time series (2015 to 2022), Chl-a consistently exhibited maxima in August (> 5 mg·m^{-3}) (Figure 3A). *Dinophysis* that was continuously present on the Galician coast throughout the study period, reached peak in cell density values more frequently in April and August (Figure 3B), generally aligning with the annual Chl-a peaks (Figure 4). Seasonal high Chl-a within the timeframe from March to November (light gray rectangle in Figure 4), slightly exhibited distinct annual patterns over the months. Spring Chl-a peaks occurred from March to April, during the second annual peak, Chl-a values generally persisted into the summer, while, in some years such as 2021 and 2022, *Dinophysis* biomass showed a greater magnitude as a second peak in late fall/summer (July – August). *Dinophysis* presented a different timing than *Pseudo-nitzschia*. Its peaking periods correspond to those of elevated Chl-a levels within the sampling timeframe (2015-2022), likely to *Dinophysis* mixotrophic behavior and a higher availability of food. Specifically, these periods encompass high concentrations (> 500 cells·L^{-1}) around the spring and autumn peaks of the phytoplankton community (annual Chl-a peaks) (Figure 4).

Pseudo-nitzschia spp. displayed two annual peaks (> 2·10^5 cells·L^{-1}) in May and August (Figure 3C). In general, during the period from late July – early August, a considerably pronounced peak was observed following the initial annual Chl-a peak (Figure 4). Slightly similar, *A. minutum* tended to be more abundant in late spring (May and June). *A. minutum* did not show any clear seasonal pattern and demonstrated a large interannual variability. A notable increase in occurrence and magnitude of this species was observed after 2018, with a pronounced surge in 2018 (June – July), 2020 (May – June), and 2022 (August – September), which was not detected in 2015 and 2016 in the Rías Baixas (Figures 3D, 4). In contrast to the *A. minutum* and the other two genera, *G. catenatum* reached maximum densities in August and remained high until October, even when the phytoplankton community had already entered the senescent phase. The largest occurrences were in 2017 and 2018, decreasing after these two recurrent years and resurging in 2022 (Figures 3E, 4).

Overall, among the four analyzed genera capable of toxin production, the chain-forming *Pseudo-nitzschia* spp. was the most abundant genus in the Rías Baixas and together with *Dinophysis* spp. also the most persistent in the period 2015-2022. This potentially neurotoxic diatom showed higher densities (> 2·10^5 cells·L^{-1}) during late spring-summer (May, July, and August), i.e., out of phase of the main peak of the phytoplankton bloom. Chl-a was usually lower than 5 mg·m^{-3} during peaks of *Pseudo-nitzschia* spp. (Figure 3A). This temporal pattern highlights that the spring Chl-a peaks frequently precede the peaks in cell density of *Pseudo-nitzschia* spp. These findings indicate that among the four studied groups, *Pseudo-nitzschia* was not the dominant genus during the
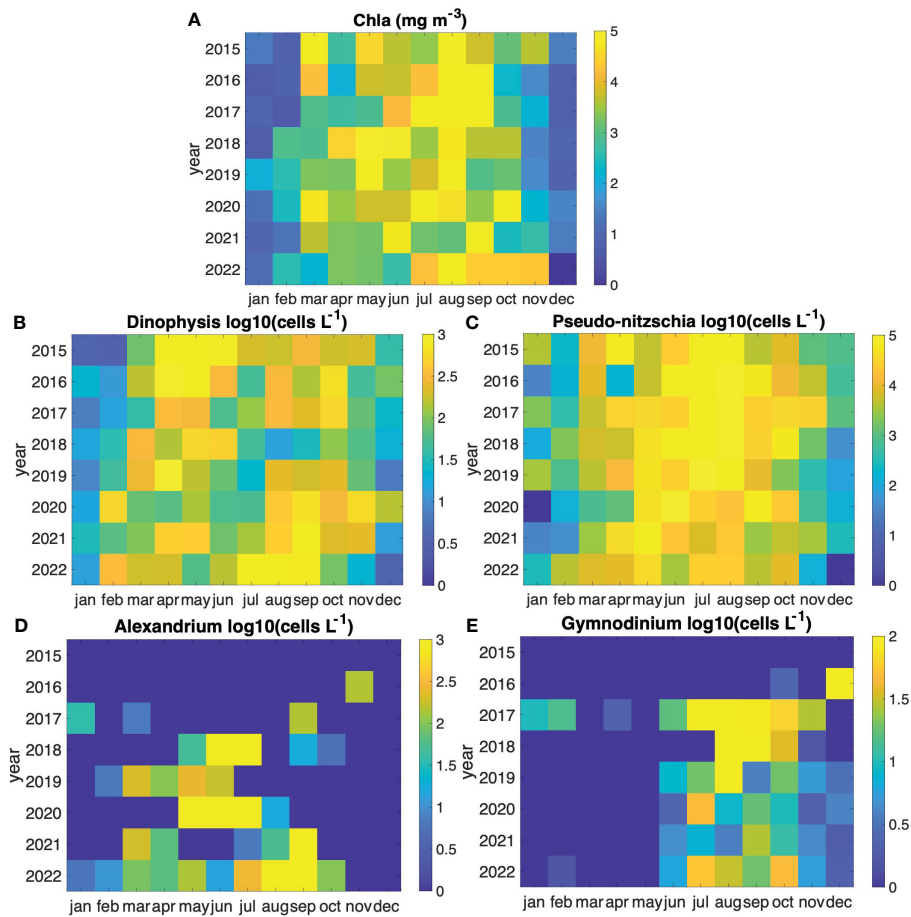
FIGURE 3
Heatmaps showing the eight-year temporal distribution of the **(A)** chlorophyll-a concentration (Chla in mg·m^{-3}), and cell densities (in cells·L^{-1} and expressed in logarithm base 10) of the **(B)** *Dinophysis* spp., **(C)** *Pseudo-nitzschia* spp, **(D)** *Alexandrium minutum* and **(E)** *Gymnodinium catenatum*. Be aware of the need to discern the color scale variations corresponding to each genus's cell density magnitude.
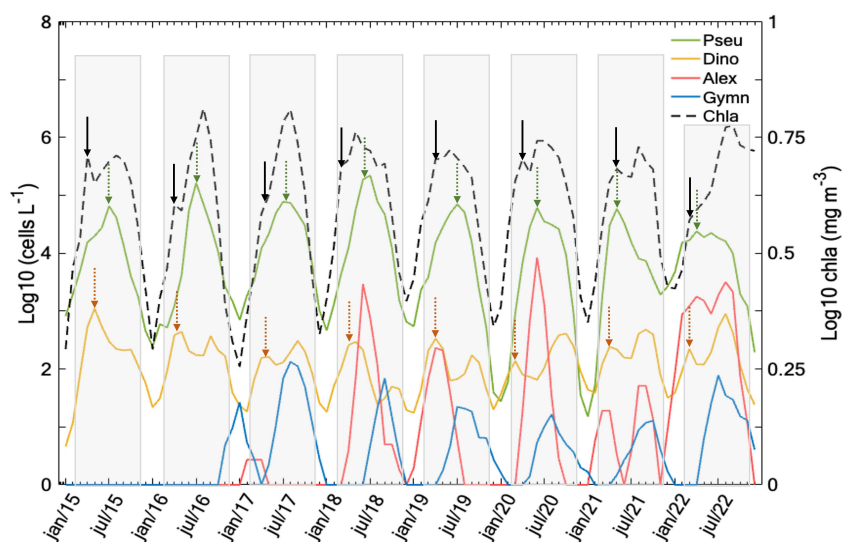

FIGURE 4
Time series of Chl-a (in mg·m^{-3}, right y-axis), and cell densities (in cells·L^{-1}, left y-axis in log10) of each harmful phytoplankton genera. Seasonal cycles are shown in the light gray rectangle, solid black arrows and dashed arrows represent the position of the first annual peak of Chl-a, *Dinophysis* spp. (orange), and *Pseudo-nitzschia* spp. (green), respectively.

highest Chl-a period and has the potential to bloom outside the annual Chl-a peaks (Figure 3C).

3.2 Environmental drivers of harmful phytoplankton

Canonical Correspondence Analysis (CCA) is a powerful tool to uncover the ecological drivers shaping species distributions and unravel the complex relationships between species and their environment. The Monte Carlo F-ratio test showed that the explanatory variables helped to explain the distribution patterns of the potentially toxigenic phytoplankton (p-value < 0.01). The multivariate analysis CCA demonstrated that the combined environmental variables collectively explained 93.4% of the temporal variability in the four groups of phytoplankton (72% and 21.4% along axes 1 and 2, respectively). Notably, the variables temperature, salinity, Chl-a, river flow, MLD, and UI exhibited the most substantial influence on the variability in cellular densities of the analyzed genera (Figure 5; Table 2). MLD showed a strong inverse correlation with river flow, and UI a strong direct correlation with Chl-a. As trends and anomalies in climatic conditions in the Rías Baixas can affect the prevalence and intensity of HABs (Nogueira et al., 2022), Figure 6 represents a visual exploratory assessment of the main scenarios corresponding to climate change. For example, an increase in river flow or a change in the intensity of the upwelling.

Dinophysis spp. exhibited high densities under conditions of deep MLD (~30 m), moderate river flow (~200 $m^3 \cdot s^{-1}$), Chl-a around 1 $mg \cdot m^{-3}$, and downwelling processes (UI negative) (Figures 6A, B). *Pseudo-nitzschia* spp. showed elevated densities

in conditions of high-water column stability (MLD < 5m), moderate river flow (~200 $m^3 \cdot s^{-1}$), high Chl-a (> 1 $mg \cdot m^{-3}$), and upwelling events (positive UI) (Figures 6C, D). Likewise, *A. minutum* displayed greater cellular densities under intermediate conditions compared to those of *Dinophysis* and *Pseudo-nitzschia*, such as moderate MLD (< 8 m), river flow of ~ 200 $m^3 \cdot s^{-1}$, and Chl-a ~ 1 $mg \cdot m^{-3}$, yet in favorable conditions for the downwelling process (negative UI) (Figures 6E, F). In contrast, *G. catenatum*, with the lowest cellular density and less regular occurrence, seems to be higher in very low MLD (~ 10 m), higher river flow (> 200 $m^3 \cdot s^{-1}$), high Chl-a (> 1 $mg \cdot m^{-3}$), and UI values favoring upwelling relaxation process (intermediate UI values) (Figures 6G, H).

In this study, GAMs applied over the 7-year time series (2015 to 2022) elucidated 47%, 31%, 15%, and 15% of the cell density variability for *Pseudo-nitzschia* spp., *Dinophysis* spp., *A. minutum*, and *G. catenatum*, respectively (Table 1; Supplementary Table 1). *Pseudo-nitzschia* and *Dinophysis* were the genera that the GAM analysis most effectively clarified in terms of abundance variability concerning environmental variables: river discharge, Chl-a, temperature, UI, and salinity, across the three estuaries. *A. minutum* and *G. catenatum* exhibited a relatively low number of occurrences (298 and 277, respectively out of a total of 6358) (Table 1; Supplementary Table 1), rendering the models less effective in explaining the temporal variability dynamics and drivers of these organisms.

The GAMs demonstrated satisfactory performance showing a strong correlation between observed and modeled data: 0.6 for the temporal abundance of *Dinophysis* spp., 0.9 for *Pseudo-nitzschia* spp., 0.5 for *Alexandrium minutum*, and 0.7 for *Gymnodinium catenatum* (Figure 6). The best GAM for *Dinophysis* included a total of eight explanatory variables: salinity, latitude, month,
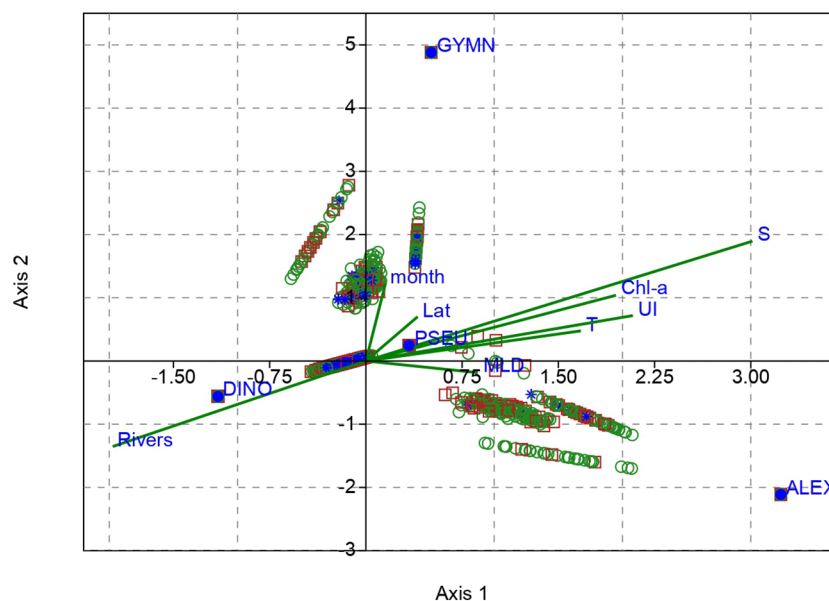

FIGURE 5
Canonical correspondence analysis diagram showing the influence of environmental variables: month, latitude (Lat), salinity (S), temperature (T), riverine inputs (Rivers), mixed layer depth (MLD), chlorophyll-a concentration (Chl-a), and upwelling intensity (UI) on the contribution of phytoplankton genera *Pseudo-nitzschia* spp. (PSEU), *Dinophysis* spp. (DINO), *Alexandrium minutum* (ALEX), and *Gymnodinium catenatum* (GYMN). Red squares: Ría Vigo samples; green circles: Ría Pontevedra samples, and blue stars: Ría Arousa samples.

TABLE 2 Factor loadings (correlation coefficients) of environmental variables with canonical roots estimated by canonical correspondent analysis.

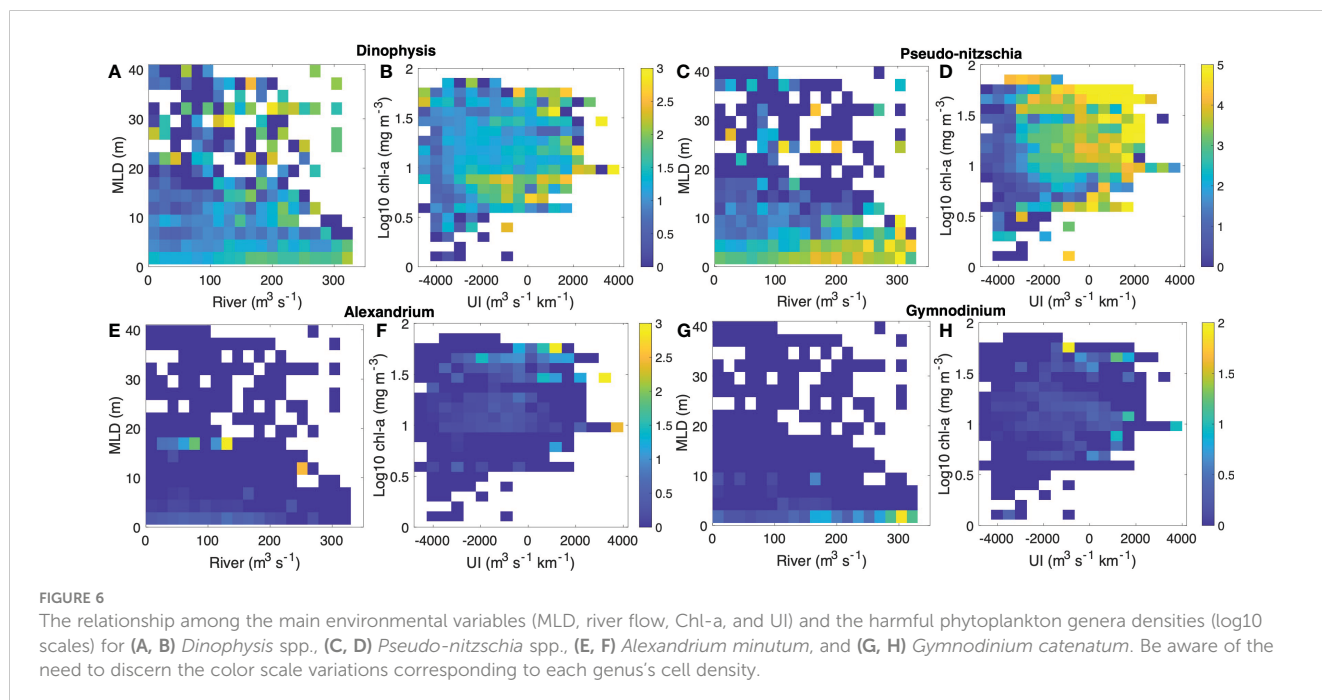| Parameter	First canonical roots	Second canonical roots
Salinity	0.32	0.20
Temperature	0.18	0.05
Chl-a	0.20	0.11
UI	0.22	0.08
MLD	0.09	-0.02
Rivers flow	-0.20	-0.14
Month	0.02	0.13
Latitude	0.04	0.07

temperature, river flow, Chl-a, UI, and MLD, which described 25% of the total deviance (Table 1; Supplementary Table 1), with latitude, month, temperature, and river flow as the most important predictors (r^2 of 0.14, 0.1, 0.07, 0.05, respectively). The GAM for *Dinophysis* exhibited a slight shift in their peaks, but overall, it demonstrated reasonable proficiency in capturing the period of elevated cellular densities occurring predominantly in July (Figure 7A; Supplementary Figure S2). The GAM for *Pseudo-nitzschia* described 47% of total deviance (Table 1; Supplementary Table 1), with seven most significantly predictors: month, Chl-a, salinity, temperature, river flow, and UI, contributing in favorable conditions to increase the cell density, indicating the seasonal distribution (r^2 of 0.37, 0.23, 0.23, 0.15, 0.12, 0.10, respectively). For *Pseudo-nitzschia*, there was a satisfactory model performance and fit, describing a trend of higher magnitude and occurrence of seasonal peaks in August, with limited interannual variability in the

seasonal blooming component (Figure 7B; Supplementary Figure S3). It appears that the model effectively captures the strong seasonal blooming component in the dynamics of *Pseudo-nitzschia*, with limited interannual variability.

The GAMs described 16% and 50% of total deviance for *Alexandrium minutum* and *Gymnodinium catenatum* (Figures 7C, D), respectively (Table 1; Supplementary Table 1), with eight significant predictors: salinity, temperature, river flow, MLD, UI, Chl-a, month, and latitude. However, given the low occurrence of these two species, these results need to be taken with caution. The high rate of absence of *A. minutum* and *G. catenatum* cells has meant that the sporadic occurrences of these species have not been adequately explained, which is insufficient to explain their dynamics (r^2 of 0.15 for both species). Months, UI, MLD, and river flow were the most important terms for *A. minutum* cell abundance (r^2 of 0.06, 0.05, 0.03, 0.03, respectively). As well as river flow, months, and salinity were the most important terms for *G. catenatum* cell abundance (r^2 of 0.07, 0.06, 0.05, respectively).

4 Discussion

The concurrent occurrence of environmental conditions during spring (April – June) and autumn (September – October), characterized by extended periods of reduced upwelling (low upwelling index), upper-layer thermal stratification (elevated sea surface temperature), and declining continental runoff, revealed the initiation and progression of significant harmful algal bloom dominated by *Dinophysis*, *Pseudo-nitzschia*, or *A. minutum* in the surface waters of the Pontevedra and Vigo estuaries. The results underscore that GAMs effectively elucidated the density variability of potentially toxic genera (*Pseudo-nitzschia* and *Dinophysis*) in relation to environmental variables such as river flow, Chl-a, temperature, and UI.

FIGURE 6
The relationship among the main environmental variables (MLD, river flow, Chl-a, and UI) and the harmful phytoplankton genera densities (log10 scales) for (A, B) *Dinophysis* spp., (C, D) *Pseudo-nitzschia* spp., (E, F) *Alexandrium minutum*, and (G, H) *Gymnodinium catenatum*. Be aware of the need to discern the color scale variations corresponding to each genus's cell density.
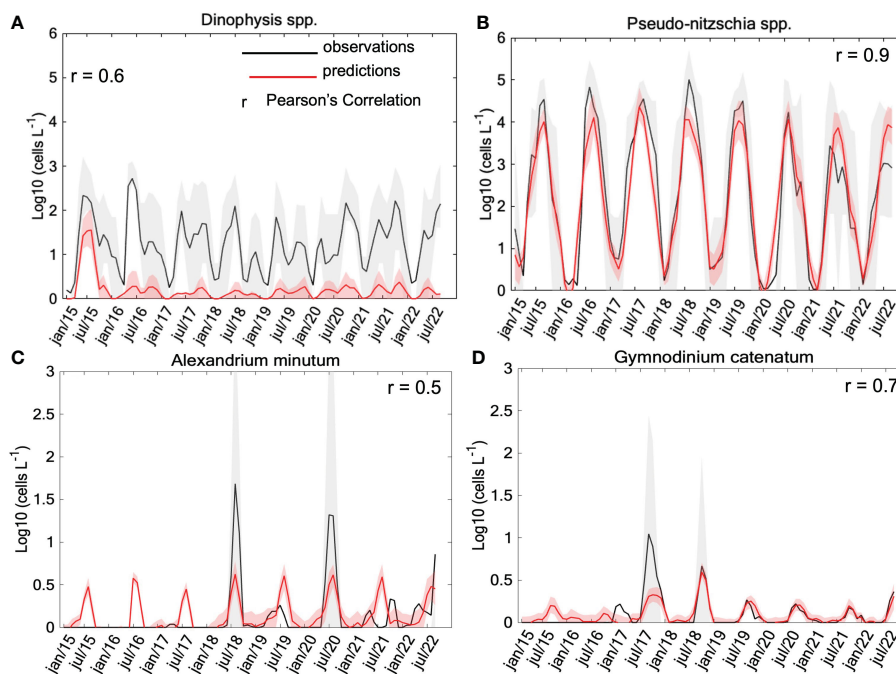
FIGURE 7
Density time series of the two most abundant HAB genera and two toxic dinoflagellates species: seasonal cycles for the **(A)** *Dinophysis* spp. and **(B)** *Pseudo-nitzschia* spp., **(C)** *Alexandrium minutum* and **(D)** *Gymnodinium catenatum*. Black and red lines represent observations and predictions, respectively. Pearson's correlations are presented in the upper left corner **(A, C, D)** and right upper corner **(B)**.

Stimulated by nutrient injection during the upwelling event, the total biomass of the phytoplankton community (Chl-a) attained its peak concentration in early spring (March-April) and late summer (August-September) (Figure 4). The highest Chl-a in the Ría Arousa, while showing the lowest concentration of the four studied groups, suggests that other phytoplankton genera were dominant. Previous studies reported other large diatoms co-occurring during the first Chl-a annual peak, such as *Detonula pumila* (Velo-Suárez et al., 2008; Díaz et al., 2014), while the second annual peak is usually dominated by smaller diatoms, usually *Chaetoceros* spp. (Díaz et al., 2014). Currently, *in-situ* monitoring in the region focuses solely on the identification of species potentially capable of producing toxins. However, to better understand phytoplankton dynamics and ecological succession, it is imperative to incorporate information not only from potentially harmful species but also from dominant genus and its density in the phytoplankton community in order to identify microplankton assemblages that will allow us to advance in the prediction of toxic species.

Large chain-forming diatoms are abundant during upwelling phases, whereas dinoflagellates and ciliates gain greater importance during relaxation and downwelling events (González-Gil et al., 2010; Díaz et al., 2016). The relaxation events of both upwelling and downwelling phases are transitional oceanographic features that promote phytoplankton blooms (Comesaña et al., 2021). Understanding the temporal dynamics of these events is crucial for predicting when a potentially toxic genus is likely to encounter favorable conditions for growth. These events occur during the rest of the year and within each season in response to dominant

southerly winds and short-time variations in the wind regime (Froján et al., 2014).

The diatoms group comprises several diverse and distinct genera. While diatoms usually exhibit robust nutrient assimilation and growth rates, *Pseudo-nitzschia* displays comparatively lower rates compared to other diatom genera (Lampe et al., 2018). For this reason, with the fertilization at the base of the euphotic layer at the early upwelling event, large cells of diatom species initiate growth, and *Pseudo-nitzschia* is less likely to occur due to its low competitiveness in relation to other diatom genera (Kelly et al., 2023). However, when considering the succession of species within the diatom group, *Pseudo-nitzschia* boasts superior nutrient absorption efficiency due to their cell shape (pennate) with a larger surface-volume area. This characteristic gives *Pseudo-nitzschia* greater efficiency in surviving in environments with decreasing availability of essential nutrients (Kelly et al., 2023), particularly when large cells of diatoms with a smaller surface-volume area are unable to maintain their growth rates (Lampe et al., 2018). In addition, some species of *Pseudo-nitzschia* have a major competitive advantage over other species in the phytoplankton community, as it can synthesize the domoic acid toxin, as a defense compound (Harðardóttir et al., 2019). Its synthesis is stimulated mainly under grazing pressure from zooplankton and competition for nutrients with other phytoplankton groups (Clark et al., 2019).

The large peak of *A. minutum* during July 2018 in surface waters of the Pontevedra and Vigo estuaries (Figure 4) was previously documented with cell density reached up to 10^5 cells·L^{-1}, causing reddish water discoloration (Nogueira et al., 2022). This unusually

intense event of *A. minutum* bloom in the Ría Vigo was triggered by several environmental conditions, such as intense continental runoff and increased insolation providing stabilization in the upper layer, which created favorable conditions during an extended period (late June to all of July) for the development of the *Alexandrium minutum* (Nogueira et al., 2022). In addition, during this season, upwelling dynamics drive the lift-up pycnocline and enhance the temperature gradient, confining the population to a well-lit stable layer. Thus, Nogueira et al. (2022) asserted that this bloom was associated with high temperature, strong vertical stratification, and extremely high river flow, somewhat akin to the findings in this study. Our results indicated that an increase in *A. minutum* cell density occurred under moderate MLD, river flow of ~ 200 $m^3 \cdot s^{-1}$, Chl-a ~ 1 $mg \cdot m^{-3}$, and downwelling phases. Additionally, the absence/no-detection of *A. minutum* in the *in-situ* time series before 2016 could be attributed to the fact that blooms of *A. minutum* typically develop inside embayments characterized by enhanced stratification, restricted circulation, and the accumulation of resting cysts in spring and summer, along with moderate positive upwelling indices (Blanco et al., 1985; Bravo et al., 2010; Nogueira et al., 2022; references therein). Our sampling stations are not located inside embayments, and the distribution pattern of *A. minutum* across the estuaries suggests a regional tendency of simultaneous occurrence with *Pseudo-nitzschia*, particularly in the inner Ría Pontevedra and central Ría Vigo areas. This co-occurrence is observed under comparable environmental conditions marked by increased water column stability (MLD < 8m) and Chl-a concentrations approximately at 1 $mg \cdot m^{-3}$ (Figures 6C–F). Our findings indicate that *A. minutum* is the third most abundant among the four studied targets, commonly observed in the shallow regions within the bays of the Rías Baixas (Blanco et al., 1985; Bravo et al., 2010; Nogueira et al., 2022; Rodríguez et al., 2023). However, the number of *A. minutum* occurrence records have been steadily increasing since 2018, nearly reaching the same magnitude as *Pseudo-nitzschia*. Most recently, in late April 2023, a similar episode took place with an extensive red tide of *A. minutum* in the inner part of the Ría Pontevedra. This trend has been causing concern and mobilizing both the scientific and economic communities toward an effective coastal monitoring strategy.

Concerning *Gymnodinium catenatum*, it represents the least frequent of the studied phytoplankton groups in the Rías Baixas and occurs in relatively low densities in the late summer. In this study, this dinoflagellate species was observed in specific environmental contexts characterized by a deeper upper mixing layer (MLD approximately 10 m), increased river discharge flow (200 $m^3 \cdot s^{-1}$), and Chl-a concentrations surpassing 1 $mg \cdot m^{-3}$ (Figures 6G, H), typical of late summer conditions. Indeed, this toxic dinoflagellate genus has been reported to appear in Galician waters under specific conditions driven by a pattern dominated by physical parameters during autumn-winter coinciding with the upwelling relaxation (Bravo et al., 2010). The blooms of *G. catenatum* have been associated with wind-driven advection of shelf populations that grow inside the estuaries (Crespo et al., 2006; Bravo et al., 2010).

Observed seasonal patterns of higher Chl-a suggest an ecological succession of diatom genera during upwelling events marked by elevated Chl-a (Díaz et al., 2014), subsequently an increase in *Pseudo-nitzschia* abundance. The genera's seasonal succession of the

phytoplankton community within ecological niches is governed by resource availability and the physiological adaptations of each phytoplankton genus in response to physical factors (such as turbulence leading to light limitation), chemical factors (including essential nutrients), and biological factors (such as grazing) (Behrenfeld et al., 2021). *Pseudo-nitzschia* growth, which is able to create brownish discolored seawater depending on its cell concentration (Zapata et al., 2011), is governed by upwelling events, silicate levels, and low competitive ability over other diatom genera that normally have faster growth rates (Velo-Suárez et al., 2008; Palenzuela et al., 2019), supporting the findings of this study. Our results show that UI plays a significant role as one of the most important predictors for cell abundance, contributing to the increase in cell density and explaining 11% of the deviance. Notably, in regions such as the West Coast of the USA, where *Pseudo-nitzschia* is a common harmful bloom former, prolonged blooms have been associated with the declining high-nutrient phase after upwelling events (Trainer et al., 2010; Sandoval-Belmar et al., 2023). In the southern estuaries of Galicia, higher abundances of *Pseudo-nitzschia* generally appear during the relaxation-upwelling conditions (Díaz et al., 2014). Maximum cell densities of this genera tend to occur associated with high stratification during low tide, higher salinity values, and lower $Si(OH)^4/N$ ratios (Díaz et al., 2014).

Dinophysis and *Pseudo-nitzschia* are commonly displayed as co-occurring genera with vertical distribution patterns (Kat, 1979; Peperzak et al., 1996, along with referenced works). Usually, the persistence of *Pseudo-nitzschia* abundance coincides with the duration of upwelling events. Alternatively, it gives way to *Dinophysis*, as observed in the Santa Barbara Channel, USA (Anderson et al., 2011). Our findings showed that *Dinophysis* was associated with downwelling and relaxation-downwelling events (negative UI), high Chl-a, and deeper upper mixed layer (Figures 6A, B). Conversely to *Pseudo-nitzschia*, *Dinophysis* never creates discolored seawater. This dinoflagellate genus acts as an obligatory mixotroph, dependent on light and nutrients for sustained growth (Anderson et al., 2011; Hansen et al., 2013), along with available prey such as ciliates and/or pico- and nano flagellates (e.g., *Mesodinium* species and cryptophytes). As a consequence, enhanced Chl-a levels result in increased predation pressure exerted by *Dinophysis* on the phytoplankton community (González-Gil et al., 2010). The interaction of regional hydrodynamics significantly regulates the occurrences of *Dinophysis* and *Pseudo-nitzschia* blooms within the Rías Baixas (Díaz et al., 2014). Furthermore, the annual reoccurrence of *Dinophysis* and *Pseudo-nitzschia* elevated cell densities is a prominent phenomenon in Galicia, playing a substantial role in enforcing shellfish harvesting constraints within Europe primary mussel production region (Davidson et al., 2021).

While *Gymnodinium catenatum* is relatively less recurrent in the southern estuaries of Galicia, both *G. catenatum* and *A. minutum* are known to form resting cysts during their sexual cycle (Bolch et al., 1991; Anderson, 1998). Cyst-beds have been suggested to facilitate the re-establishment of the vegetative population and contribute to the species' extended distribution (Anderson and Wall, 1978; Steidinger and Haddad, 1981). The potential for an increase in the frequency and intensity of *A. minutum* and *G. catenatum* blooms in the Rías Baixas exists in

the coming years, attributed to the formation of resting cyst granules and the likely recurrence of the climatic scenario that favors these unusual and intense events.

Trends and anomalies in climatic conditions in the Rías Baixas can affect the prevalence and intensity of HABs (Álvarez-Salgado et al., 2008; Pérez et al., 2010). Phytoplankton community structure and function are impacted and altered by changes in sea temperature, either directly by affecting group-specific growth rates, or indirectly by modifying water column stratification (Hallegraeff et al., 2021; Kennish et al., 2023), as we have noticed in the Rías Baixas (Figure 6). As climate change is expected to significantly alter sea temperature, phytoplankton communities are expected to suffer major impacts. Expected changes in precipitation regimes, which can alter freshwater discharges and water column salinity, can profoundly impact not only phytoplankton communities but also food webs via cascading effects, biogeochemical cycles, and aquatic habitat quality, including HABs (Kennish et al., 2023). For example, an elevated occurrence of rainy days was observed in late spring of 2018 (May to July), attributed to the more frequent passage of frontal weather systems (Nogueira et al., 2022). During this period, high temperatures and feeble winds can become more frequent. These changes may had reduced the upwelling intensity in NW Iberia and likely provide stronger haline/thermal stratification in the upper layers in the southern estuaries of Galicia (Álvarez-Salgado et al., 2008; Cruz et al., 2021; Favareto et al., 2023), favoring the occurrence of HABs (Bode et al., 2009; Trainer et al., 2010; Nogueira et al., 2022).

Our study, focusing on the spatio-temporal distribution of four potentially toxic phytoplankton groups, suggests that the evolution of climate change conditions may increasingly benefit the occurrence of *Pseudo-nitzschia* and *Dinophysis* blooms in specific areas along the Rías Baixas in the upcoming years. Additionally, it is likely that *Alexandrium minutum* and *Gymnodinium catenatum* blooms, characterized by the formation of resistant cysts, will become more frequent in more sheltered regions of the Rías Baixas bays.

The areas with the highest susceptibility to blooms are primarily located at the mouths of the Ría Pontevedra and in the central and outer zones of the Ría Vigo. The Ría Arousa displayed the lowest cellular densities, yet with elevated Chl-a values proximate to the river mouths (Figure 2). The causes and dynamics of HABs across different genera remain elusive as a result of complex and simultaneous environmental conditions influencing their occurrence and physiological factors governing their succession. To understand the interaction between physical and biological factors in spatial-temporal distribution, this study identified a sequential pattern in the occurrence of harmful genera, driven by favorable conditions. Notably, there was a distinct trend wherein the peak growth of *Dinophysis* precedes the environmentally conducive conditions for the subsequent growth of *Pseudo-nitzschia* (Figures 7A, B).

Climate-driven changes suggest that HAB blooms in NW Spain could be more frequent and also be magnified when combined with marine heatwaves (Boivin-Rioux et al., 2022; Clark et al., 2022). Consequently, this scenario implies a need for intensified monitoring of genera producing biotoxins. Even though remote sensing data is recognized as fundamental in spatio-temporal environmental studies, many monitoring HAB networks still did not incorporate that

synoptic information within operative activities. Urgent measures, including enhanced engagement by remote sensing experts, are needed to address these conditions, particularly within the Ría Vigo, the river mouths of the Ría Pontevedra, and the outer regions of both estuaries. For instance, on April 27th, 2023, a dense *A. minutum* bloom observed in the field was successfully detected through satellite imagery, enabling the study of the spatial structure of the bloom (Supplementary Figure 1C). These results demonstrate the capacity to identify punctual patches and localized spots in high-risk locations susceptible to blooms, such as those caused by *A. minutum*, *Noctiluca scintillans* (Detoni et al., 2023), or diatoms (e.g., *Pseudo-nitzschia*).

In-situ sampling is punctual, does not cover large spatial extensions, and occurs only once a week, potentially missing any blooms that may occur in between. Employing ocean color remote sensing data for monitoring HAB events effectively complements observation-based monitoring programs at fixed stations (Detoni et al., 2023). However, inherent challenges in detecting and monitoring HABs in physically complex systems, such as the Rías Baixas, include obtaining free-cloud images with high spatial and temporal resolution during the occurrence of a bloom, along with the need for appropriate atmospheric and sunglint corrections (Spyrakos et al., 2011). Moreover, while satellite data can detect the presence of a bloom, the specific taxonomic information that can be obtained from multi-spectral images is limited (Gernez et al., 2023). For example, on October 2nd, 2017, an extensive phytoplankton bloom was detected by the high spatial resolution Sentinel-2 satellite (Supplementary Figure 1B), but it still remains attributed to an unidentified organism. Therefore, with the aim of improving remote sensing efforts, this study identified zones and temporal windows with significant HAB occurrences in the Rías Baixas and the likelihood of genus causing them, as influenced by ecological succession and environmental drivers. This will assist in achieving synergy between *in-situ* measurements and satellite acquisitions in upcoming research.

5 Conclusions

Climate trends provide a favorable scenario for HAB proliferations in the near future, including those of *Alexandrium minutum*, *Dinophysis*, and *Pseudo-nitzschia*. In this study, we found that high *Dinophysis* abundances could precede increased *Pseudo-nitzschia* levels. Furthermore, we suggest that persistent thermal stratification in the upper layers, weakening upwelling period, and enhanced discharge river flow in the Rías Baixas might induce changes in the abundance dynamics of *Dinophysis*, *Pseudo-nitzschia*, and *A. minutum*. These changes could pose a threat to aquaculture industries and ecosystem health in the Rías Baixas during seasons that were not identified previously. In contrast, *Gymnodinium catenatum* was relatively less recurrent in the Rías Baixas during the analyzed period (2015 – 2022).

This study demonstrated that the environmental predictors associated with seasonal variation, such as salinity, temperature, UI, and river discharge flow, might successfully explain the presence of two major harmful phytoplankton genera (*Pseudo-nitzschia* and *Dinophysis*) in the Rías Baixas. The enhanced growth of *Dinophysis*, *Pseudo-nitzschia*, and *A. minutum*, mainly in the inner part of the Ría Vigo, the river

mouth of the Ría Pontevedra, and offshore of both estuaries was due to a combination of environmental conditions during late spring (June) and late summer (August). These conditions included persistent periods of weakening upwelling (low upwelling index), thermal stratification in the upper layers (shallow mixed layer depth), as well as enhanced continental runoff. With this information, it is possible to increase efforts to acquire satellite images and subsequent adequate processing for the detection of each of these genera. Therefore, early warning systems can be improved to avoid losing aquaculture resources during long periods of closure of the rafts caused by the presence of toxins in the shellfish. In addition, this study may help to provide both mechanistic and holistic perspectives on toxic phytoplankton blooms in the dynamic and changing coastal ocean, where cells interact simultaneously with multiple altered environmental variables.

Data availability statement

The original contributions presented in the study are included in the article/Supplementary Material, further inquiries can be directed to the corresponding author/s.

Author contributions

AD: Writing – original draft, Writing – review & editing. GN: Funding acquisition, Supervision, Writing – review & editing. XP: Funding acquisition, Supervision, Writing – review & editing. ER-R: Writing – review & editing. MLZ: Writing – review & editing. YP: Writing – review & editing. IC: Writing – review & editing.

Funding

Acknowledgments

Conflict of interest

The authors declare that the research was conducted in the absence of any commercial or financial relationships that could be construed as a potential conflict of interest.

Publisher's note

Supplementary material

The Supplementary Material for this article can be found online at: https://www.frontiersin.org/articles/10.3389/fmars.2024.1330090/full#supplementary-material

SUPPLEMENTARY TABLE 1
Summary results for the parametric coefficients and smooth terms of the final GAMs selected. Estimated degrees of freedom (e.d.f.).

SUPPLEMENTARY FIGURE 1
(A) HAB occurrences as observed by satellite in the study area, where the black and red rectangles correspond to the areas of satellite images (B, C), respectively. (B) Sentinel-2 image from 02/10/2017 displayed in quasi-true color (R: 705 nm, G: 560 nm, B: 490 nm), processed using ACOLITE atmospheric correction. Bright yellow filaments correspond to a phytoplankton bloom of a non-identified genus. (C) Sentinel-2 image from 27/04/2023, "Top-of-atmosphere" reflectance, capturing an *Alexandrium minutum* bloom in tiny bright red color.

SUPPLEMENTARY FIGURE 2
Dinophysis spp. model. Partial plots showing the effects (as fitted splines) of the significant predictors (*x*-axis) on the cell abundance. Dashed lines are 95% confidence intervals. Short vertical lines located on the *x*-axes of each plot indicate the values at which samplings were carried out.

SUPPLEMENTARY FIGURE 3
Pseudo-nitzschia spp. model. Partial plots showing the effects (as fitted splines) of the significant predictors (*x*-axis) on the cell abundance. Dashed lines are 95% confidence intervals. Short vertical lines located on the *x*-axes of each plot indicate the values at which samplings were carried out.

References

Akaike, H. (1974). A new look at the statistical model identification. *IEEE Trans. Automat. Contr.* 19, 716–723. doi: 10.1109/TAC.1974.1100705

Álvarez, I., Prego, R., deCastro, M., and Varela, M. (2012). Galicia upwelling reviste: out-of-season events in the rias, (1967-2009). *Cienc Mar.* 38, 143–159. doi: 10.7773/cm.v38i1B.1776

Álvarez-Salgado, X. A., Gago, J., Míguez, B. M., Gilcoto, M., and Pérez, F. F. (2000). Surface waters of the NW Iberian margin: Upwelling on the shelf versus outwelling of upwelled waters from the Rías Baixas. *Estuar. Coast. Shelf Sci.* 51, 821–837. doi: 10.1006/ecss.2000.0714

Álvarez-Salgado, X. A., Labarta, U., Fernández-Reiriz, M. J., Figueiras, F. G., Rosón, G., Piedracoba, S., et al. (2008). Renewal time and the impact of harmful algal blooms on the extensive mussel raft culture of the Iberian coastal upwelling system (SW Europe). *Harmful Algae.* 7, 849–855. doi: 10.1016/J.HAL.2008.04.007

Anderson, D. M. (1998). "Physiology and bloom dynamics of toxic *Alexandrium* species, with emphasis on life cycle transitions," in *Physiological Ecology of Harmful Algal Blooms*. Eds. D. M. Anderson, A. D. Cembella and G. M. Hallegraeff (Verlag, Berlin-Heidelberg: Springer), 29–48.

Anderson, C. R., Berdalet, E., Kudela, R. M., Cusack, C. K., Silke, J., O'Rourke, E., et al. (2019). Scaling up from regional case studies to a global harmful algal bloom observing system. *Front. Mar. Sci.* 6. doi: 10.3389/fmars.2019.00250

Anderson, C. R., Kudela, R. M., Benitez-Nelson, C., Sekula-Wood, E., Burrell, C. T., Chao, Y., et al. (2011). Detecting toxic diatom blooms from ocean color and a regional ocean model. *Geophys Res. Lett.* 38, L04603. doi: 10.1029/2010GL045858

Anderson, D. M., and Wall, D. (1978). Potential importance of benthic cysts of Gonyaulax tamarensis and G. excavata in initiating toxic dinoflagellate blooms. *J. Phycol.* 14 (2), 224–234. doi: 10.1111/j.1529-8817.1978.tb02452.x

Arístegui, J., Barton, E. D., Álvarez-Salgado, X. A., Santos, A. M. P., Figueiras, F. G., Kifani, S., et al. (2009). Sub-regional ecosystem variability in the Canary Current upwelling. *Prog. Oceanogr.* 83, 33–48. doi: 10.1016/j.pocean.2009.07.031

Behrenfeld, M. J., Boss, E. S., and Halsey, K. H. (2021). Phytoplankton community structuring and succession in a competition-neutral resource landscape. *ISME Commun.* 1, 12. doi: 10.1038/s43705-021-00011-5

Blanco, J., Mariño, J., and Campos, M. J. (1985). *In toxic dinoflagellates*. Eds. D. M. Anderson, A. W. White and D. G. Baden (New York: Elsevier), pp. 79–84.

Bode, A., Alvarez-Ossorio, M. T., Cabanas, J. M., Miranda, A., and Varela, M. (2009). Recent trends in plankton and upwelling intensity off Galicia (NW Spain). *Prog. Oceanogr.* 83, 342–350. doi: 10.1016/j.pocean.2009.07.025

Boivin-Rioux, A., Starr, M., Chassé, J., Scarratt, M., Perrie, W., Long, Z., et al. (2022). Harmful algae and climate change on the Canadian East Coast: Exploring occurrence predictions of Dinophysis acuminata, D. norvegica, and Pseudo-nitzschia seriata. *Harmful Algae.* 112, 102183. doi: 10.1016/j.hal.2022.102183

Bolch, C. J., Blackburn, S. I., Cannon, J. A., and Hallegraeff, G. M. (1991). The resting cyst of the red-tide dinoflagellate Alexandrium minutum (Dinophyceae). *Phycologia.* 30 (2), 215–219. doi: 10.2216/i0031-8884-30-2-215.1

Bravo, I., Fraga, S., Figueroa, R. I., Pazos, Y., Massanet, A., and Ramilo, I. (2010). Bloom dynamics and life cycle strategies of two toxic dinoflagellates in a coastal upwelling system (NW Iberian Peninsula). *Deep-Sea Res. I: Oceanogr. Res.* 57, 222–234. doi: 10.1016/j.dsr2.2009.09.004

Carvalho, L., Mackay, E. B., Cardoso, A. C., Baattrup-Pedersen, A., Birk, S., Blackstock, K. L., et al. (2019). Protecting and restoring Europe's waters: An analysis of the future development needs of the Water Framework Directive. *Sci. Total Environ.* 658, 1228–1238. doi: 10.1016/J.SCITOTENV.2018.12.255

Clark, S., Hubbard, K. A., Anderson, D. M., McGillicuddy, D. J., Ralston, D. K., and Townsend, D. W. (2019). Pseudo-nitzschia bloom dynamics in the Gulf of Maine: 2012–2016. *Harmful Algae.* 88, 101656. doi: 10.1016/j.hal.2019.101656

Clark, S., Hubbard, K. A., Ralston, D. K., McGillicuddy, D. J., Stock, C., Alexander, M. A., et al. (2022). Projected effects of climate change on Pseudo-nitzschia bloom dynamics in the Gulf of Maine. *J. Mar. Syst.* 230, 103737. doi: 10.1016/j.jmarsys.2022.103737

Comesaña, A., Fernández-Castro, B., Chouciño, P., Fernández, E., Lema-Fuentes, A., Glicoto, M., et al. (2021). Mixing and phytoplankton growth in an upwelling system. *Front. Mar. Sci.* 8. doi: 10.3389/fmrs.2021.712342

Crespo, B. G., Figueiras, F. G., Porras, P., and Teixeira, I. G. (2006). Downwelling and dominance of autochthonous dinoflagellates in the NW Iberian margin: The example of the Ría de Vigo. *Harmful Algae.* 5, 770–781. doi: 10.1016/j.hal.2006.03.006

Cruz, E. R., Nolasco, R., Padin, X. A., Gilcoto, M., Babarro, J. M. F., Dubert, J., et al. (2021). A High-Resolution Modeling Study of the Circulation Patterns at a Coastal Embayment: Ría de Pontevedra (NW Spain) Under Upwelling and Downwelling Conditions. *Front. Mar. Sci.* 8. doi: 10.3389/fmars.2021.661250

Davidson, K., Whyte, C., Aleynik, D., Dale, A., Gontarek, S., Kurekin, A. A., et al. (2021). HABreports: online early warning of harmful algal and biotoxin risk for the Scottish shellfish and finfish aquaculture industries. *Front. Mar. Sci.* 8. doi: 10.3389/fmars.2021.631732

DeCastro, M., Gómez-Gesteira, M., Prego, R., Taboada, J. J., Montero, P., Herbello, P., et al. (2000). Wind and tidal influence on water circulation in a Galician ria (NW Spain). *Estuarine Coast. Shelf Sci.* 51 (2), 161–176. doi: 10.1006/ecss.2000.0619

Detoni, A. M. S., Navarro, G., Garrido, J. L., Rodríguez, F., Hernández-Urcera, J., and Caballero, I. (2023). Mapping dinoflagellate blooms (Noctiluca and Alexandrium) in aquaculture production areas in the NW Iberian Peninsula with the Sentinel-2/3 satellites. *Sci. Total Environ.* 868, 161579. doi: 10.1016/j.scitotenv.2023.161579

Díaz, P. A., Ruiz-Villarreal, M., Pazos, Y., Moita, T., and Reguera, B. (2016). Climate variability and Dinophysis acuta blooms in an upwelling system. *Harmful Algae.* 53, 145–159. doi: 10.1016/j.hal.2015.11.007

Díaz, P. A., Ruiz-Villarreal, M., Velo-Suárez, L., Ramilo, I., Gentien, P., Lunven, M., et al. (2014). Tidal and wind-event variability and the distribution of two groups of Pseudo-nitzschia species in an upwelling-influenced Ría. *Deep Sea Res. 2 Top. Stud. Oceanogr.* 101, 163–179. doi: 10.1016/j.dsr2.2013.09.043

Escalera, L., Reguera, B., Moita, T., Pazos, Y., Cerejo, M., Cabanas, J. M., et al. (2010). Bloom dynamics of Dinophysis acuta in an upwelling system: *in situ* growth versus transport. *Hamrful Algae.* 9, 312–322. doi: 10.1016/j.hal.2009.12.002

Fariñas, T. H., Ribeiro, L., Soudant, D., Belin, C., Bacher, C., Lampert, L., et al. (2017). Contribution of benthic microalgae to the temporal variation in phytoplankton assemblages in a macrotidal system. *J. Phycol.* 53, 1020–1034. doi: 10.1111/jpy.12564

Favareto, L., Brotas, V., Rudorff, N., Zacarias, N., Tracana, A., Lamas, L., et al. (2023). Response of phytoplankton to coastal upwelling: The importance of temporal and spatial scales. *Limnol. Oceanogr.* 68, 1376–1387. doi: 10.1002/lno.12353

Fernandes-Salvador, J. A., Davidson, K., Sourisseau, M., Revilla, M., Schmidt, W., Clarke, D., et al. (2021). Current status of forecasting toxic harmful algae for the North-East Atlantic shellfish aquaculture industry. *Front. Mar. Sci.* 8. doi: 10.3389/fmars.2021.666583

Figueiras, F. G., Labarta, U., and Fernández Reiriz, M. J. (2002). Coastal upwelling, primary production and mussel growth in the Rías Baixas of Galicia. in. *Hydrobiologia.* 484, 121–131. doi: 10.1023/A:1021309222459

Figueiras, F. G., Teixeira, I. G., Froján, M., Zúñiga, D., Arbones, B., and Castro, C. G. (2020). Seasonal variability in the microbial plankton community in a semi enclosed bay affected by upwelling: the role of a nutrient trap. *Front. Mar. Sci.* 7. doi: 10.3389/fmars.2020.578042

Froján, M., Arbones, B., Zúñiga, D., Castro, C. G., and Figueiras, F. G. (2014). Microbial plankton community in the Ría de Vigo (NW Iberian upwelling system): Impact of the culture of Mytilus galloprovincialis. *Mar. Ecol. Prog. Ser.* 498, 43–54. doi: 10.3354/meps10612

Gernez, P., Zoffoli, M. L., Lacour, T., Fariñas, T. H., Navarro, G., Caballero, I., et al. (2023). The many shades of red tides: Sentinel-2 optical types of highly-concentrated harmful algal blooms. *Remote Sens. Environ.* 287, 113486. doi: 10.1016/j.rse.2023.113486

González-Gil, S., Velo-Suárez, L., Gentien, P., Ramilo, I., and Reguera, B. (2010). Phytoplankton assemblages and characterization of a Dinophysis acuminata population during an upwelling-downwelling cycle. *Aquat. Microbial Ecol.* 58, 273–286. doi: 10.3354/ame01372

González-Nuevo, G., Gago, J., and Cabanas, J. M. (2014). Upwelling index: a powerful tool for marine research in the NW Iberian upwelling system. *J. Oper. Oceanogr* 7 (1), 47–57. doi: 10.1080/1755876X.2014.11020152

Hallegraeff, G. M., Anderson, D. M., Belin, C., Bottein, M.-Y. D., Bresnan, E., Chinain, M., et al. (2021). Perceived global increase in algal blooms is attributable to intensified monitoring and emerging bloom impacts. *Commun. Earth Environ.* 2, 117. doi: 10.1038/s43247-021-00178-8

Hansen, P. J., Nielsen, L. T., Johnson, M., Berge, T., and Flynn, K. J. (2013). Acquired phototrophy in Mesodinium and Dinophysis – A review of cellular organization, prey selectivity, nutrient uptake and bioenergetics. *Harmful Algae.* 28, 126–139. doi: 10.1016/J.HAL.2013.06.004

Harðardóttir, S., Wohlrab, S., Hjort, D. M., Krock, B., Nielsen, T. G., John, U., et al. (2019). Transcriptomic responses to grazing reveal the metabolic pathway leading to the biosynthesis of domoic acid and highlight different defense strategies in diatoms. *BMC Mol. Biol.* 20 (7), 2–14. doi: 10.1186/s12867-019-0124-0

Hoagland, P., and Scatasta, S. (2006). "The economic effects of harmful algal blooms," in *Ecology of Harmful Algae*. Ecological Studies, Vol. 189. Eds. E. Granéli and J. T. Turner (Berlin: Springer-Verlag Berlin Heidelberg), 391–402. doi: 10.1007/978-3-540-32210-8_30

Johansen, R. A., Reif, M. K., Saltus, C. L., and Pokrzywinski, K. L. (2022). *A Review of Empirical Algorithms for the Detection and Quantification of Harmful Algal Blooms Using Satellite-Borne Remote Sensing*. Available at: https://erdclibrary.on.worldcat.org/discovery.

Kat, M. (1979). "The occurrence of Prorocentrum species and coincidental gastrointestinal illness of mussel consumers," in *Toxic dinoflagellate blooms*. Eds. D. L. Taylor and H. H. Seliger (Amsterdam: Elsevier), 215–220.

Kelly, K. J., Mansour, A., Liang, C., Kim, A. M., Mancini, L. A., Bertin, M. J., et al. (2023). Simulated upwelling and marine heatwave events promote similar growth rates

but differential domoic acid toxicity in Pseudo-nitzschia australis. *Harmful Algae.* 127, 102467. doi: 10.1016/j.hal.2023.102467

Kennish, M. J., Paerl, H. W., and Crosswell, J. R. (2023). *Climate Change and Estuaries. 1st ed.* (Boca Raton: CRC Press). doi: 10.1201/9781003126096

Labarta, U., and Fernández-Reiriz, M. J. (2019). The Galician mussel industry: Innovation and changes in the last forty years. *Ocean Coast. Manag.* 167, 208–218. doi: 10.1016/J.OCECOAMAN.2018.10.012

Lampe, R. H., Cohen, N. R., Ellis, K. A., Brulandt, K. W., Maldonado, M. T., Peterson, T. D., et al. (2018). Divergent gene expression among phytoplankton taxa in response to upwelling. *Environ. Microbiol.* 20 (8), 3069–3082. doi: 10.1111/1462-2920.14361

Legendre, P., and Legendre, L. (1998). *Numerical Ecology. 2nd English Edition* (Amsterdam: Elsevier Science).

Martinez-Vicente, V., Kurekin, A., Sá, C., Brotas, V., Amorim, A., Veloso, V., et al. (2020). Sensitivity of a satellite algorithm for harmful algal bloom discrimination to the use of laboratory bio-optical data for training. *Front. Mar. Sci.* 7. doi: 10.3389/fmars.2020.582960

Neveux, J., and Panouse, M. (1987). Spectrofluorometric determination, of chlorophylls and pheophytins. *Arch. Hydrobiol.* 109, 567–581. doi: 10.1127/archiv-hydrobiol/109/1987/567

Nogueira, E., Bravo, I., Montero, P., Díaz-Tapia, P., Calvo, S., Ben-Gigirey, B., et al. (2022). HABs in coastal upwelling systems: Insights from an exceptional red tide of the toxigenic dinoflagellate Alexandrium minutum. *Ecol. Indic.* 137, 108790. doi: 10.1016/j.ecolind.2022.108790

Nogueira, E., Pérez, F. F., and Ríos, A. F. (1997). Seasonal patterns and long-term trends in an estuarine upwelling ecosystem (Ria de Vigo, NW Spain). *Estuar. Coast. Shelf Sci.* 44 (3), 285–300. doi: 10.1006/ecss.1996.0119

Otero, P., Ruiz-Villarreal, M., Peliz, Á., and Cabanas, J. M. (2010). Climatology and reconstruction of runoff time series in northwest Iberia: influence in the shelf buoyancy budget off Ría de Vigo. *Sci. Mar.* 74, 247–266. doi: 10.3989/scimar.2010.74n2247

Palenzuela, J. M. T., Vilas, L. G., Bellas, F. M., Garet, E., González-Fernández, vÁ., and Spyrakos, E. (2019). Pseudo-nitzschia blooms in a coastal upwelling system: Remote sensing detection, toxicity and environmental variables. *Water (Switzerland).* 11, 1954. doi: 10.3390/w11091954

Pardo, P. C., Padín, X. A., Gilcoto, M., Farina-Busto, L., and Pérez, F. F. (2011). Evolution of upwelling systems coupled to the long-term variability in sea surface temperature and Ekman transport. *Clim Res.* 48, 231–246. doi: 10.3354/cr00989

Peperzak, L. G., Snoeijer, J., Dijkema, W., Gieskes, W. W. C., Joordens, J., Peeters, J. C. H., et al. (1996). "Development of Dinophysis acuminata bloom in the river Rhine plume (North Sea)," in *Harmful and toxic algal blooms.* Eds. T. Yasumoto, Y. Oshima and Y. Fukuyo (Intergovernmental Oceanographic Commission of UNESCO: Sendai Kyodo Printing Co, Ltd), 273–276.

Pérez, F. F., Padín, X. A., Pazos, Y., Gilcoto, M., Cabanas, M., Pardo, P. C., et al. (2010). Plankton response to weakening of the Iberian coastal upwelling. *Glob. Change Biol.* 16 (4), 1258–1267. doi: 10.1111/j.1365-2486.2009.02125.x

R Core Team. (2012). *R: A language and environment for statistical computing.* (Vienna, Austria: R Foundation for Statistical Computing). Available at: http://www.r-project.org/.

Rodríguez, F., Escalera, L., Reguera, B., Nogueira, E., Bode, A., Ruiz-Villarreal, M., et al. (2023). Red tides in the Galician rías: historical overview, ecological impact, and future monitoring strategies. *R. Soc. Chem. Environ. Sci.: Process Impacts* 26, 16–34. doi: 10.1039/d3em00296a

Rodríguez, G. R., Villasante, S., and do Carme García-Negro, M. (2011). Are red tides affecting economically the commercialization of the Galician (NW Spain) mussel farming? *Mar. Policy.* 35 (2), 252–257. doi: 10.1016/j.marpol.2010.08.008

Sandoval-Belmar, M., Smith, J., Moreno, A. R., Anderson, C., Kudela, R. M., Sutula, M., et al. (2023). A cross-regional examination of patterns and environmental drivers of Pseudo-nitzschia harmful algal blooms along the California coast. *Harmful Algae.* 126, 102435. doi: 10.1016/j.hal.2023.102435

Scatasta, S., Stolte, W., Granéli, E., Weikard, H. P., and van Ierland, E. (2003). *The socio-economic impact of harmful algal blooms in European marine waters and description of future risks*. ECOHARM project, 6 FP, EU. Environ Nat Resour Group, Wageningen Univ, Wageningen, NL, The Netherlands. Available at: http://www.bom.hik.se/ecoharm/index.html.

Spyrakos, E., González Vilas, L., Torres Palenzuela, J. M., and Barton, E. D. (2011). Remote sensing chlorophyll a of optically complex waters (rias Baixas, NW Spain): Application of a regionally specific chlorophyll an algorithm for MERIS full resolution data during an upwelling cycle. *Remote Sens. Environ.* 115, 2471–2485. doi: 10.1016/j.rse.2011.05.008

Steidinger, K. A., and Haddad, K. (1981). Biologic and hydrographic aspects of red tides. *Bioscience.* 31 (11), 814–819. doi: 10.2307/1308678

Tilstone, G. H., Figueiras, F. G., and Fraga, F. (1994). Upwelling–downwelling sequences in the generation of Red Tides in a coastal upwelling system. *Mar. Ecol. Prog. Ser.* 112, 241–253. doi: 10.3354/meps112241

Trainer, V. L., Pitcher, G. C., Reguera, B., and Smayda, T. J. (2010). The distribution and impacts of harmful algal bloom species in eastern boundary upwelling systems. *Prog. Oceanogr.* 85, 33–52. doi: 10.1016/j.pocean.2010.02.003

Velo-Suárez, L., González-Gil, S., Gentien, P., Lunven, M., Bechemin, C., Fernand, L., et al. (2008). Thin layers of Pseudo-nitzschia spp. and the fate of Dinophysis acuminata during an upwelling-downwelling cycle in a Galician Ría. *Limnol. Oceanogr.* 53, 1816–1834. doi: 10.4319/lo.2008.53.5.1816

Wood, S. N. (2000). Modelling and smoothing parameter estimation with multiple quadratic penalties. *J. R Stat. Soc. Ser. B Stat. Methodol.* 62, 413–428. doi: 10.1111/1467-9868.00240

Wood, S. N. (2006). *Generalized Additive Models: An Introduction with R.* (London: Chapman and Hall, CRC). doi: 10.1201/9781315370279

Wood, S. N. (2017). *Generalized Additive Models. An introduction with R.* (Boca Raton, Florida USA: CRC Press). doi: 10.1201/9781315370279

Zapata, M., Rodríguez, F., Fraga, S., Barra, L., and Ruggiero, M. V. (2011). Chlorophyll c pigment patterns in 18 species (51 strains) of the genus Pseudo-nitzschia (Bacillariophyceae). *J. Phycol.* 47 (6), 1274–1280. doi: 10.1111/j.1529-8817.2011.01055.x

Zohdi, E., and Abbaspour, M. (2019). Harmful algal blooms (red tide): a review of causes, impacts and approaches to monitoring and prediction. *Int. J. Environ. Sci. Technol.* 16, 1789–1806. doi: 10.1007/s13762-018-2108-x